Spin-nematic order in the frustrated pyrochlore-lattice quantum rotor model

Karol Gregor, David A. Huse, and S. L. Sondhi
Department of Physics, Princeton University, Princeton, New Jersey 08544, USA
(Received 31 January 2006; revised manuscript received 17 May 2006; published 26 July 2006)

As an example of ordering due to quantum fluctuations, we examine the nearest-neighbor antiferromagnetic quantum $O(n)$ rotor model on the pyrochlore lattice. Classically, this system remains disordered even at zero temperature; we find that adding quantum fluctuations induces an ordered phase that survives to positive temperature, and we determine how its phase diagram scales with the coupling constant and the number of spin components. We demonstrate, using quantum Monte Carlo simulations, that this phase has long-range spin-nematic order, and that the phase transition into it appears to be first order.

DOI: 10.1103/PhysRevB.74.024425 PACS number(s): 75.10.−b, 75.50.Ee, 75.10.Jm, 75.40.Cx

I. INTRODUCTION

Ordering of antiferromagnetic spins on geometrically frustrated lattices is a subtle problem.[1,2] In some of the most frustrated cases, the canonical nearest-neighbor antiferromagnetic interaction fails to produce a unique classical ground state ordering pattern. Thus low temperature ordering in such systems must be attributed to additional interactions or to selection via thermal or quantum fluctuations, the latter phenomena being termed order by disorder.

In recent years there has been much interest in antiferromagnetism on the pyrochlore lattice of corner-sharing tetrahedra, Fig. 1.[3] The classical statistical mechanics of the purely nearest-neighbor problem is now fairly well understood. It is known[4] that XY spins order, by disorder, collinearly[5] while Ising, Heisenberg, and higher-dimensional spins do not order even in the zero temperature limit. The correlations of this set of cooperative paramagnets have been found to exhibit a universal dipolar form characteristic of an underlying gauge field,[6] truncated by a correlation length that diverges as $T \to 0$.

While thermal fluctuations thus do not lead to ordering in the Heisenberg problem, there is much work arguing that quantum fluctuations do lead to ordering at low temperatures, for the case of Heisenberg spins. Close to the classical limit, this conclusion follows from arguments based on the $1/S$ expansion discussed recently by Henley.[7] Henley derives an effective Hamiltonian on the space of classical ground states which captures the effects of the zero point energy of harmonic spin waves in a loop expansion. This indicates a selection of collinear ground states with a large unit cell and a residual degeneracy that is of order $O(L)$, where L is the linear size of the sample. It is expected that a nonlinear treatment of the spin waves will lift this remaining degeneracy and predict long-range spin order in a particular collinear configuration. In the opposite limit of small spins and large quantum fluctations, there is a set of investigations principally of the $S=1/2$ case, starting with the pioneering work of Harris *et al.*[8–13] which suggest a breaking of the inversion and translation symmetries of the lattice with only short range order among the spins. For $S=1$ Yamashita *et al.*[14] have also argued for a breaking of inversion symmetry as well as long-range order in the transverse component of the spin chirality. Two large N studies[15,16] have also suggested symmetry breaking for small spin values. Indeed Ref. 16 finds that the quantum dimer model that arises in a large N treatment does indeed break inversion symmetry and has further translational symmetry breaking via an order by disorder mechanism.

In this paper we further explore the impact of quantum fluctuations on spins on the pyrochlore lattice by endowing them with the dynamics of quantum rotors instead. The resulting problems, which are readily defined for $O(n)$ symmetric spins for all n, are distinct from the Heisenberg spin problems even at $n=3$, although there is clearly a family resemblance which detailed analysis will bear out. The rotor models are interesting in their own right[17] and their $n=1$ representative is the transverse field Ising model which has been studied on a variety of frustrated lattices.[18]

The Hamiltonian for the quantum rotor model on the pyrochlore lattice is given by

$$H = g\sum_i \vec{L}_i^2 + \sum_{\langle i,j\rangle} \vec{S}_i \cdot \vec{S}_j, \tag{1}$$

where $\vec{S}_i$ is a unit vector in n dimensions located at site i, $\vec{L}_i$ is its associated angular momentum, and the second sum goes over all nearest-neighbor pairs of sites on the pyrochlore lattice. The coupling constant g measures the strength of quantum fluctuations.

At any n and in the limit of large coupling constant g, the ground state has all rotors in their zero angular momentum state, and thus no long-range correlations or symmetry breaking. In this limit there is also a gap of $O(g)$ so this

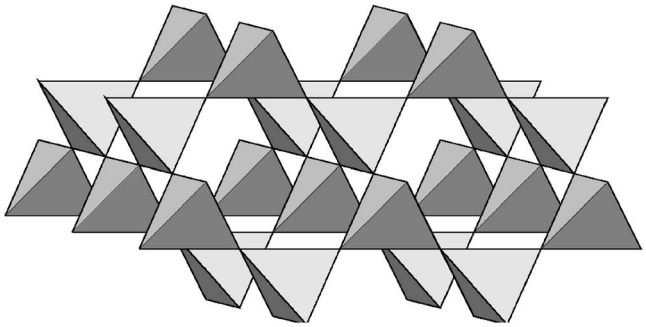

FIG. 1. Pyrochlore lattice

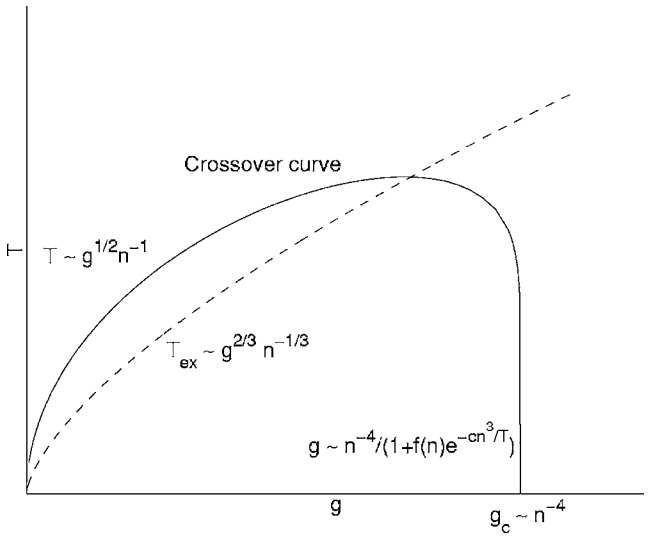

FIG. 2. Schematic crossover diagram of a single tetrahedron, with the scalings with g, T, and n indicated. The solid line is where the system crosses over from being collinear to disordered, while the dashed line shows the value of g where, for a given T, the deviations from collinearity are minimized. The solid line is also a very approximate phase transition curve for the full pyrochlore lattice. However we expect that the curve starting at g_c will bend initially to the right due to the entropy of the spin waves that exist in the ordered phase.

quantum paramagnetic phase is stable for a range of values of g.[19] The opposite limit of $g=0$ is the classical model, which has a highly degenerate ground state and, for $n>2$, dipolar correlations in the zero-temperature limit but no significant strength in any Fourier component of the magnetization.[4,6]

The problem at hand is to understand how the system interpolates between these two very different disordered limits. In the following we report progress on this question. Primarily we will show that the system develops spin-nematic (collinear) long-range order for a finite range of values of $g \in (0, g_c)$ at $T=0$. More generally we derive the schematic phase diagram in the temperature-coupling constant plane shown in Fig. 2 with the various scalings that we have derived indicated. We have not been able to establish or exclude further symmetry breaking at the lowest temperatures into a state with long-range spin order. We do however offer analytic evidence (for the case $n=3$) that such further symmetry breaking is likely quite weak.

We turn next to understanding the quantum mechanics of the building block of the pyrochlore lattice, the single tetrahedron. The basic results derived here will next enable us to deduce the existence of nematic order on the full lattice and the scalings of various energy scales with n. Thereafter we describe results of a simulation for the $n=3$ problem and conclude with a discussion of the $1/n$ expansion for this problem and a summary.

We note that the quantum mechanics of rotors is different from the quantum mechanics of spins and therefore the type of analysis and the results in the two cases are different in some important respects. As an example, consider four antiferromagnetically coupled spins S on a tetrahedron. In a ground state two of the spins add to $S'=0,\ldots,2S$ and the other two add to the same value so that the ground state, which has total spin zero, can be obtained. The limiting distribution as $S\to\infty$ has significant weight at all values of S' and thus the four spins do not order in a collinear configuration. In contrast, as we show below, four quantum rotors on a single tetrahedron can order collinearly.

II. SINGLE TETRAHEDRON

In this section we analyze the basic unit of the pyrochlore lattice—a single tetrahedron. It consists of four mutually coupled spins and its Hamiltonian is

$$H = g\sum_{i=1}^{4} \vec{L}_i^2 + \sum_{1\leqslant i<j\leqslant 4} \vec{S}_i \cdot \vec{S}_j. \tag{2}$$

This may also be viewed as a system of four interacting particles, each moving on the surface of a sphere in n dimensions. The first term in H is their kinetic energy, while the second term is a repulsive interaction potential.

In the classical limit of $g=0$ it is known[4] that for $n=2$ (XY spins) the spins order collinearly in the zero T limit—two spins pointing in one direction and the other two in the opposite direction.[20] On the other hand, for $n>2$ the spins remain disordered even in the $T\to 0$ limit as we review below. In the rest of this section we show that in the quantum case ($g>0$) for any n there are ways to take the $g\to 0$ and $T\to 0$ limits that give collinearly ordered spins. Furthermore, we find the dependence of the crossover from ordered to disordered spin states as a function of g, T, and n, as indicated in Fig. 2.

A. Classical spins $g=0$

We start by describing the configurations of the spins and the classical ground states (CGS). The spins are in a CGS if the potential is minimized; this is when the four spins add up to zero. This implies that in a CGS, the fourth spin lies in the three-dimensional space spanned by the other three spins. Thus the ground states can be parametrized by two angles θ and ϕ as shown in Fig. 3, plus an overall rotation in spin space. θ gives the deviation of all spins from collinearity, while ϕ is the angle between the planes in spin space spanned by each pair of spins. All four spins in a CGS are at the same angle θ from the reference axis; the reference axis that minimizes θ is used in our convention of parameterizing these ground states. Mostly we will consider nearly collinear states with small θ.

For both the classical and the quantum analysis, we need to consider the matrix of second derivatives of the potential energy with respect to the orientations of the four spins at a given classical ground state. There are $4(n-1)$ degrees of freedom in the system and n constraints in a ground state. The eigenmodes with zero eigenvalues of this matrix generically lie along the directions of the ground state since the potential there is constant. Therefore there are $3n-4$ eigenmodes with zero eigenvalue and n eigenmodes with nonzero eigenvalue around a generic point of CGS. As can be

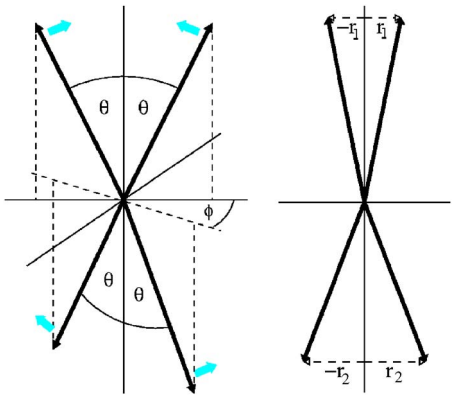

FIG. 3. (Color online) Left, parametrization of the classical ground states of a single tetrahedron, showing the orientations of the four spins and the reference axis. All the spins are at angle θ from the reference axis. The short arrows indicate the mode that goes soft as the spins become collinear. The line with no arrows is the reference axis in spin space that we measure θ from. Right, when the spins are nearly collinear, the space of low-energy configurations that includes the soft mode may be parameterized by the two small displacements away from collinearity, $\vec{r}_1$ and $\vec{r}_2$.

checked by explicit calculation, for small θ, $n-1$ of the latter modes have eigenvalues of order one, while the remaining one is a "soft mode" with its eigenvalue proportional to θ^2. This last mode corresponds to the spin deviation away from the nearly collinear CGS that decreases θ for one pair of nearly parallel spins and increases it for the other pair, as indicated in Fig. 3. This soft mode's stiffness is independent of the other angle ϕ.

At low temperature, the classical system at equilibrium can be approximated as occupying the states with potential energy within k_BT of the ground state and not those at higher potential. Due to the soft mode, the number of such states near an almost collinear CGS is proportional to T/θ (for $T < \theta^4$). For $n=2$, this concentration of the accessible states near $\theta=0$, due to the one mode that softens there, causes the "order by disorder" effect and the spins order collinearly in the $T\to 0$ limit. But the number of CGS with a given θ is proportional to $\theta^{2(n-2)}$, due to the freedom of rotations about the reference axis. This means that the probability density of θ behaves as $\sim\theta^{(2n-5)}$ at small θ. Thus for $n>2$ the collinear states do not dominate even in the zero temperature limit, and the classical spins remain disordered.

B. Quantum ground state, $g>0$

Here we show that for small g the ground state wave function is localized around the collinear state and we obtain the scaling with g and n of its spread, its energy and the energy of the lowest excited states. First we present a "power-counting" variational argument, which is valid when n is large.

We treat the quantum zero-point energy of the motion normal to the manifold of classical ground states as that of harmonic oscillators. For small θ, there are $(n-1)$ "stiff" oscillators, each with zero point energy $\sim\sqrt{g}$, and the one soft mode, with zero point energy $\sim\theta\sqrt{g}$. The latter produces a θ-dependent effective potential that lifts the degeneracy within the set of classical ground states and has a minimum at $\theta=0$. We are interested in characterizing the ground state and the excited states in this potential.

The set of classical ground states for a given reference axis constitutes a $(2n-3)$-dimensional manifold that intersects with itself at the collinear states where $\theta=0$. The angle θ is proportional to the distance from this intersection. Each pair of nearly parallel spins may be rotated about the reference axis. These latter rotations give $2(n-2)$ dimensions of motion. One can also rotate the reference axis, which gives the remaining $(n-1)$ dimensions of motion. In the ground state, these reference-axis degrees of freedom are in the zero total angular momentum eigenstate and we will generally ignore them in this section of the paper.

Thus we consider a variational wave function that is localized near $\theta=0$, spreading in angle by γ in each direction on the $(2n-3)$-dimensional manifolds near the collinear state. The kinetic energy, given by a sum of terms of the form $g\,\partial^2/\partial x_i^2$ where the x_i are coordinates on the manifold of CGS, is for such a state $\sim g(2n-3)/\gamma^2$. The typical angle θ in this state is the (Pythagorean) sum of $(n-1)$ angles of displacement away from the reference axis that are mutually perpendicular to each other and each of order γ, so $\theta \sim \gamma\sqrt{n-1}$. At the level of accuracy we are using now, $n \sim (n-1) \sim (2n-3)$, so the kinetic energy is $\sim n^2 g/\theta^2$, and the full variational energy is this plus the effective potential of $\sim\theta\sqrt{g}$. Minimizing this with respect to θ gives the following estimate for its typical value in the ground state:

$$\theta_0 \sim n^{2/3} g^{1/6}. \tag{3}$$

Thus we see that the ground state is collinear ($\theta_0 \to 0$) in the $g\to 0$ limit. The crossover from collinear ordering (small θ_0) to a strongly disordered state can be defined as occurring at $\theta_0 \sim 1$, which puts the crossover in the ground state at

$$g_c \sim n^{-4} \tag{4}$$

for large n.

The contributions to the ground state energy from the motion within the manifold of classical ground states as well as that from motion along the "soft mode" direction are

$$E_0' \sim (ng)^{2/3}. \tag{5}$$

In the former case, this energy is due to the motion in $(2n-3)$ directions, so the energy of motion in just one of these directions along the manifolds of CGS, and thus the energy to excite the motion in that direction to a higher-energy eigenstate is

$$E_{ex} \sim g^{2/3}/n^{1/3}. \tag{6}$$

There are other, lower-lying excited states that do not alter the degree of collinearity: these involve "rigid body" rotations of the ground state we are discussing, and, at even lower energy for small g, tunneling between the three distinct ways of pairing the four spins.

The above arguments have approximated the soft mode as harmonic, which is correct for the bulk of the ground state wave function in the limit of large n. However, we should

check that the g dependence that we have derived remains valid at small g even when n is small (such as for the interesting case of $n=3$). To do better at small g and small θ but general n, we combine the soft mode degree of freedom with the manifold of classical ground states, and formulate the Schrödinger equation within this space. Label the two pairs of nearly parallel spins 1 and 2 and let the displacement of one of the spins in each pair away from the reference axis be $\vec{r}_1$ and $\vec{r}_2$, respectively, Fig. 3. The other spin in each pair has precisely the opposite displacement. These displacements are $(n-1)$-dimensional vectors and, when small, their magnitudes are equal to the angles of rotation of the unit vectors. To leading order at small g and small r_i the resulting Schrödinger equation is

$$H'\psi = -2g(\nabla_1^2 + \nabla_2^2)\psi + (1/2)(r_1^2 - r_2^2)^2\psi = E'\psi. \quad (7)$$

By comparing the kinetic and potential energy terms in this Hamiltonian H', we see that indeed the characteristic scale of angle is $g^{1/6}$ and the scale of energy is $g^{2/3}$, as obtained above in the harmonic approximation. The ground state in this unusual quartic potential for large n is concentrated away from the collinear state at $r_1 \cong r_2 \sim n^{2/3}g^{1/6}$, where the harmonic approximation used before remains valid. But for small n the ground state wave function has considerable weight close to collinearity where the harmonic approximation is not appropriate. The leading correction at small g to Eq. (7) appears to be from the θ dependence of the stiffness of the other "hard" modes that were ignored. This gives a $\sim\theta^2\sqrt{g}$ contribution to the effective potential that thus contributes to the energy at order $g^{5/6}$, one order higher in our "small" parameter of $g^{1/6}$.

C. T > 0

Next we consider nonzero temperature for small g, examining the crossovers that occur, first from the fully quantum regime for $T < E_{ex}$ where the system remains in its nearly collinear ground state, to an intermediate regime $[E_{ex} < T < T_c(g) \sim g^{1/2}/(n-2)]$ where there are many thermal excitations present but it remains near collinear, and then, for $n > 2$, to the disordered regime at higher T.

The modes within the manifold of classical ground states are excited when the temperature reaches the excitation energy $T_{ex} = E_{ex} \sim g^{2/3}/n^{1/3}$. At higher temperatures, we can treat these degrees of freedom as classical. The soft mode has an excitation energy of $\sim\theta\sqrt{g}$ and this mode will be in its classical regime where it is highly excited only at angles where this is less than T. There the probability of being near a particular CGS is

$$P(\theta) \sim \frac{T}{\theta\sqrt{g}}; \quad (8)$$

this applies for $\theta_0 < \theta < T/\sqrt{g}$. For $\theta < \theta_0$, within the support of the ground state wave function, $P(\theta) \sim P(\theta_0)$. At larger angles, greater than both θ_0 and $T/\sqrt{g}$, the soft mode is in its ground state, which gives an effective energy of $\sim\theta\sqrt{g}$ and

$$P(\theta) \sim \exp(-\theta\sqrt{g}/T). \quad (9)$$

Again, the number of distinct CGS with a given θ behaves as $\sim\theta^{2(n-2)}$ at small θ, so the typical value of θ is near the maximum of $\theta^{2(n-2)}P(\theta)$. In the intermediate regime we are discussing, which is $E_{ex} < T < T_c(g) \sim g^{1/2}/(n-2)$, this maximum occurs near

$$\theta(T) \sim \frac{(n-2)T}{\sqrt{g}}. \quad (10)$$

Thus, for $n > 2$ and small T and g, the crossover to the thermally disordered state occurs at

$$T_c(g) \sim g^{1/2}/(n-2), \quad (11)$$

where $\theta(T) \sim 1$. These small g, T results apply as long as the quantum ground state is itself nearly collinear, which requires $g < n^{-4}$ and thus $T < n^{-3}$. The crossover temperature $T_c(g)$ must have a maximum of order n^{-3} and then decrease to zero at g_c, as indicated in Fig. 2.

The striking result here is that this simple system of four rotors has a nonmonotonic, or reentrant behavior at low T as one increases g from the classical limit of $g=0$ to the quantum limit of large g for $n > 2$. This is illustrated in Fig. 4. Initially at small g it is disordered due to the large entropy of the disordered states relative to the collinear states. As g is increased, the effective potential due to the soft mode increases, causing the system to be more and more confined to the nearly collinear eigenstates, as $\theta(T)$ decreases with increasing g. This trend continues until the energy E_{ex} of the excited states within the manifold of CGS increases to of order T, at which point the system is predominantly in the ground state, with $\theta_0 \sim T^{1/4}n^{3/4}$. This point, where the deviations from collinearity are minimized, occurs at $g_{\min} \sim T^{3/2}n^{1/2}$. Beyond this point, further increase of g (decrease of the "mass") causes the ground state to instead deviate more from collinearity with increasing g, until it crosses over in to the fully disordered quantum regime at g_c.

III. PYROCHLORE LATTICE

Now that we have examined the behavior of a single tetrahedron, we turn to the question of the behavior of our model on the pyrochlore lattice. This lattice consists of a three-dimensional array of corner-sharing tetrahedra, so adjacent tetrahedra share a single site. There are two aspects of the ordering that occurs in the single tetrahedron in the appropriately taken small g, T limit, namely the axis along which the spins are all collinearly aligned, and which pairs of spins are pointing which way along that axis. If two adjacent tetrahedra sharing a single spin both order, they must order along the same axis, so this "spin-nematic" order should propagate throughout the lattice. As we show below, we have found good evidence from quantum Monte Carlo simulations that the pyrochlore lattice model has a phase with long-range spin-nematic order in a region of its phase diagram with nonzero g and T. Thus the crossovers we discussed in the previous section for the single tetrahedron become true phase transitions on the full lattice. Since this is an isotropic-to-nematic phase transition with a cubic invariant in its Landau theory, this phase transition is expected to be first order, and

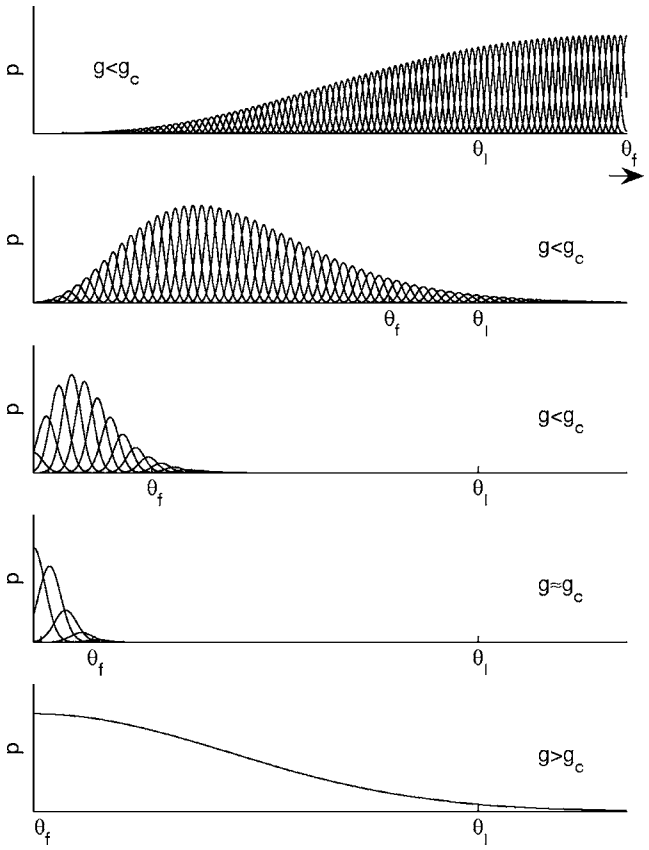

FIG. 4. Very schematic drawing of evolution of the distribution of the eigenstates and probability distributions of the angle θ at a fixed T as g is increased. The height of each peak corresponds to the probability that the system is at the given θ. The width of each peak corresponds to the spread of each eigenstate. The distribution is localized approximately up to an angle θ_f and we say that the system is localized if $\theta_f < \theta_l \sim 1$. At the top g is small, the system is noncollinear and effectively classical, occupying many excited states. As g is increased (moving down in the figure) the system becomes more collinear, and the number of different excited states occupied at equilibrium decreases. Meanwhile, the spread of θ within the ground state is always increasing as g increases. At $g_{\min}$ the excitation energy of the lowest excited state passes through T; this is where the system is most collinear. As g increases further, the spread within the ground state increases (bottom).

that expectation is indeed supported by our simulations.

The other aspect of the ordering does not strongly propagate between adjacent tetrahedra: The spin nematic order picks a particular axis in spin space, but there are six different low-energy configurations of the spins' directions along this axis for each tetrahedron. If a given tetrahedron orders in to one of these spin patterns, the adjacent tetrahedra that each share a spin with it still each have three spin patterns that remain compatible with the first tetrahedron. At this level of consideration, for the full lattice the entropy of this spin degeneracy is extensive, and the spins remain disordered, although collinear. It seems likely that this spin degeneracy is lifted to some degree by tunneling between the various spin configurations, but this is something that so far we have not detected, either analytically or in our simulations.

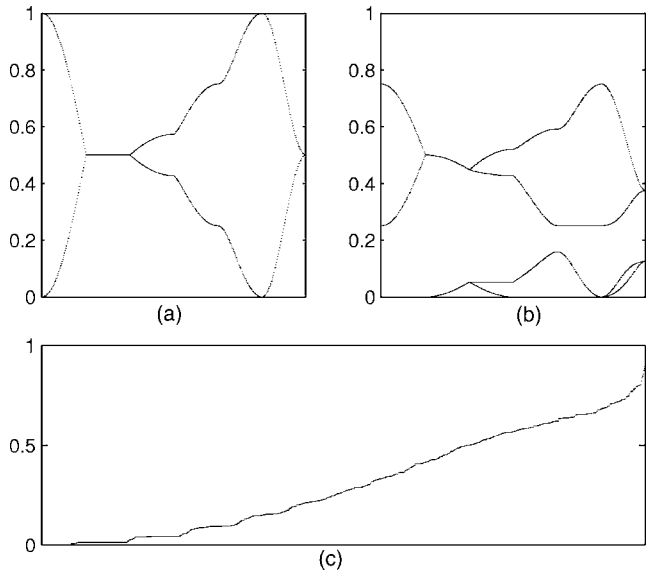

FIG. 5. The eigenvalues of the Hessian matrix of the potential evaluated at the states with (a) $\theta=0$ and (b) $\theta=0.3$ and plotted along certain chosen directions of the Brillouin zone. For small θ the eigenvalues of the two lowest bands go as $\lambda_i = k_i \theta^2$. The k_i's, ordered by their magnitude, are plotted in (c).

A. Degrees of freedom and modes

We start by reviewing the counting of the number of degrees of freedom and of constraints.[4] Let N be the number of tetrahedra. Then there are $2N$ spins and $2N(n-1)$ degrees of freedom. Each tetrahedron has zero total spin in a classical ground state; this gives Nn constraints. Thus the dimension of the set of CGS is $N(n-2)$, and hence there are $N(n-2)$ zero modes around a generic CGS configuration. However, around a fully collinear configuration there are $N(n-1)$ zero modes. Thus there are N soft modes whose stiffnesses vanish as we approach the fully collinear configuration.

For a small displacement away from the collinear configuration let θ be the average of all θ's of all spins. We will now argue that for the soft modes the associated second derivative of the potential goes as $\lambda \sim \theta^2$, just as for the single tetrahedron.

In a collinear configuration consider two directions parametrized by z_α, z_β that displace the system away from the collinear configuration parallel to a manifold of CGS. H contains no terms of the form z_α^2, z_β^2, but only term $z_\alpha^2 z_\beta^2$, higher order terms and terms containing other displacements. Let us displace the system in the β direction to say $z_{0\beta}$. Then z_α has to stay zero for the system to remain in CGS. But around the new point, the mode along the α direction would become $z_{0\beta}^2 z_\alpha^2$ and so $\lambda \sim z_{0\beta}^2 \sim \theta^2$. There are of course all the other modes that need to be taken into account but it is reasonable that this result will not change. To further check this, we expanded the potential around one particular noncollinear CGS, one in which each primitive unit cell has the same spin configuration, with the spins displaced by an angle θ from the collinear configuration. The results are shown in Figs. 5(a) and 5(b) (with $\theta=0.3$). For given n and θ the "spin-wave" bands are the union of 5(b) with $(n-2)$ copies of 5(a).

We see that two zero bands, which together contain N modes, become nonzero (except for special directions that are of measure zero). We further find that stiffnesses of these soft modes go as $\lambda \sim \theta^2$.

B. Quantum ground state

Here we show that the "power-counting" variational argument used for the single tetrahedron goes through for the full lattice with only slight modifications. We find that the ground state wave function is localized around a collinear configuration for small g and find its spread as a function of g and n.

We consider a variational wave function that is localized near $\theta=0$, spreading in angle by γ in each of the $\sim nN$ directions available to it. The kinetic energy of such a state is $\sim gnN/\gamma^2$. The typical angle θ in this state is the (Pythagorean) sum of $(n-1)$ angles of displacement that are mutually perpendicular to each other and each of order γ, so $\theta \sim \gamma\sqrt{n-1}$. The kinetic energy is $\sim Nn^2 g/\theta^2$. There are N soft modes so the potential energy is $\sim N\theta\sqrt{g}$. Minimizing the total energy with respect to θ gives the same estimate as before for its typical value in the ground state:

$$\theta_0 \sim n^{2/3} g^{1/6}. \tag{12}$$

Thus we see that the ground state is collinear ($\theta_0 \to 0$) in the $g \to 0$ limit. The crossover from collinear ordering (small θ_0) to a strongly disordered state can be defined as occurring at $\theta_0 \sim 1$, which puts the crossover in the ground state at

$$g_c \sim n^{-4} \tag{13}$$

for large n.

C. T⟩0

We would like to extend the analysis done for the tetrahedron. What is more complicated here is that the soft modes are not all the same and further they depend in some complicated way on the displacement. We found that for one particular displacement, their stiffnesses go as $\lambda_i = k_i \theta^2$ where k_i's are shown on Fig. 5(c). To proceed we are going to make the following assumption: Given some general displacement that is characterized some mean θ_{rms} of displacements of all spins, assume that this distribution of k_i's is not going to change very much, at least in a qualitative way.

The probability of finding the system in some CGS, treating the perpendicular directions in harmonic approximation is given by

$$P \sim \prod_i \frac{1}{\sinh\left(\sqrt{\lambda_i}\frac{\sqrt{g}}{T}\right)} \tag{14}$$

where the λ_i's are the eigenvalues of the matrix of the second derivatives of the potential in the perpendicular directions. With our approximations the probability of finding the system with some $\theta = \theta_{rms}$ is

$$P(\theta) \sim \prod_i \frac{\theta^{N(n-2)}}{\sinh\left(\sqrt{k_i}\theta\frac{\sqrt{g}}{T}\right)} \tag{15}$$

To find the localization, we need to find the behavior of this function. We find that for large n it is sharply peaked at

$$\theta_f = n\frac{T}{\sqrt{g}}. \tag{16}$$

To see this differentiate its logarithm with respect to θ

$$\frac{d}{d\theta}\log P(\theta) = \frac{1}{\theta}\left(N(n-2) - \sum_i \frac{\sqrt{k_i}\theta\frac{\sqrt{g}}{T}}{\tanh\left(\sqrt{k_i}\theta\frac{\sqrt{g}}{T}\right)}\right), \tag{17}$$

and analyze the resulting function for large n. The k's satisfy $0 < k_i < 1$. For $\theta\frac{\sqrt{g}}{T} \ll 1$ the second term is approximately N and so the derivative is positive and the function is increasing. For $\theta\frac{\sqrt{g}}{T} \gg 1$ for most of the values of i, the term under summation sign is approximately $\sqrt{k_i}\theta\frac{\sqrt{g}}{T}$ and so the second term is approximately $N\theta\frac{\sqrt{g}}{T}$. It is a bit smaller because $k_i < 1$ but of that order. The derivative is zero when $\theta\frac{\sqrt{g}}{T} \sim n$ and is negative for larger values of θ and so as said, the function is peaked at θ_f. Evaluating the second derivative we find that the function is sharply peaked with ratio of the width to θ_f being $\sqrt{1/Nn}$. Therefore the system is localized up to approximately θ_f just as in the case of the single tetrahedron.

As n decreases P becomes more and more distributed around zero and at $n=3$ it is only a decreasing function. Nevertheless most of its weight is still in the region approximately $< \theta_f$ and so the system is still localized approximately up to θ_f.

D. Scaling argument

The previous argument shows that the spins localize, but assumes that the distribution of k_i does not change significantly for other displacements. In this section we relax this condition and only assume that $\lambda \sim \theta^2$. We will show that if the system localizes it depends on g and T only through $\theta_0 = T/\sqrt{g}$.

We want to know the probability that the θ's have rms $\theta_{rms} = \theta_r$. This is given by

$$P(\theta_r, \theta_0) = \frac{\int \prod d\theta \left(\prod_i \sinh(\sqrt{\lambda_i(\{\theta\})}/\theta_0)\right)^{-1} \delta\left(\sqrt{\sum \theta_i^2} - \theta_r\right)}{\int \prod d\theta \left\{\prod_i \sinh[\sqrt{\lambda_i(\{\theta\})}/\theta_0]\right\}^{-1}}. \tag{18}$$

The $\int\prod d\theta$ is symbolic, it means to sum over all ground state configurations, in the neighborhood of the collinear configuration. By changing variables and using the scaling property of the eigenvalues it is easy to see that

$$cP(c\theta_r, c\theta_0) = P(\theta_r, \theta_0). \tag{19}$$

Thus the shape of P depends only on θ/θ_0 (and n). Therefore the localization depends on g, T only through θ_0.

E. Spin wave theory

We now consider a spin wave analysis, expanding to harmonic order about each collinear CGS to see if a state selection in this approximation occurs. We note that this should be asymptotically accurate at small g and that in the spin system this corresponds to the $1/S$ computation which *does* select a subset of the collinear states.[7]

A given collinear CGS can be concisely specified, up to a global rotation, by writing the spins as $\vec{S}_i = \eta_i \hat{z}$ where $\eta_i = \pm 1$. Fluctuations about such a configuration can be parametrized as $\vec{S}_i = (\vec{x}_i, \eta_i \sqrt{1-x_i^2})$ where $\vec{x}_i = (x_i^1, \ldots, x_i^{n-1})$. Expanding the square root to second order in x, the nearest-neighbor interaction can be written as

$$V = \sum_{\langle i,j \rangle} \eta_i \eta_j + \sum_{\langle i,j \rangle} \vec{x}_i \cdot \vec{x}_j + \sum_i \eta_i x_i^2 \sum_{jnni} \eta_j. \tag{20}$$

In every collinear CGS the first term is the same and the sum in the last term is $\Sigma_{j\ nn\ i} \eta_j = -2\eta_i$ which eliminates all η s from the last term. Thus the potential expanded to the second order around a given collinear configuration is completely independent of the choice of collinear configuration and therefore so is the spin wave spectrum. Hence any selection beyond collinear ordering must come from higher orders in the expansion and thus is a weaker effect than one might have guessed *a priori*.

IV. NUMERICAL SIMULATIONS

In this section we use imaginary-time path-integral quantum Monte Carlo simulations to study the ordering of our quantum rotors on the pyrochlore lattice in the Heisenberg case $n=3$. This method is based on writing the partition function as the trace over all states and inserting $N_t - 1$ additional resolutions of the identity to obtain N_t copies ("time slices") of the pyrochlore lattice model, coupled ferromagnetically along the imaginary time direction. The case of one time slice is the classical model that does not order. We find that an ordered phase does appear already in the case of two time slices, although it is restricted to very low temperature. As the number of time slices is increased, the ordered phase apparently becomes more stable.

In principle, to get the quantitatively correct behavior of our quantum Hamiltonian, we should take the continuum (Hamiltonian) limit of $N_t \to \infty$ (with the appropriate scalings of temporal and spatial couplings). However, doing this extrapolation properly is a computationally demanding task that we have not seriously attempted. Instead we have simulated primarily the case $N_t = 8$, mapping out a portion of its phase diagram and characterizing the phase transition into the spin-nematic ordered phase. We find that the ordering transition is first-order, and that the phase diagram is indeed qualitatively similar to the crossover diagram we obtained for a single tetrahedron. We expect that these conclusions are correct also in the Hamiltonian limit.

A. Quantum Monte Carlo

As mentioned above the method is derived by writing the partition function as a trace over all states and inserting $N_t - 1$ resolutions of identity. At large N_t we obtain

$$Z = \int \prod_{k,i} d\vec{n}_{k,i} e^S, \tag{21}$$

$$S = K_0 \sum_{k,i} \vec{n}_{k,i} \cdot \vec{n}_{k+1,i} - K_1 \sum_{k,\langle i,j \rangle} \vec{n}_{k,i} \cdot \vec{n}_{k,j}, \tag{22}$$

$$K_0 = \frac{N_t T}{g}, \tag{23}$$

$$K_1 = \frac{1}{N_t T}, \tag{24}$$

where $\vec{n}_{k,i}$ is a unit vector at site i in time slice k. The nearest-neighbor pairs on the pyrochlore lattice are denoted $\langle i,j \rangle$, and the relations between the couplings here and T and g are shown. In S the first term comes from the kinetic energy term and the second from the potential energy term in the original problem.

Our simulations consist of simulating this system for finite N_t which we treat as an approximation to true system obtained by taking N_t to infinity. The samples are of size N_x^3 primitive unit cells (thus $4N_x^3$ spins) in each time slice, with periodic boundary conditions.

B. Order parameter

The spin-nematic order parameter that we use is the symmetric traceless tensor

$$Q^{\alpha\beta} = \frac{1}{4N_t N_x^3} \sum_{k,i} \left(n_{k,i}^\alpha n_{k,i}^\beta - \frac{1}{3} \delta^{\alpha\beta} \right), \tag{25}$$

where α and β run over the three directions in spin space. Note this order parameter is defined as a sum over all of space and imaginary time at one instant during our simulation. To make a dimensionless combination that is sensitive to the ordering, we use the generalized "Binder ratio"

$$q_3 = \sqrt{6} \left\langle \frac{TrQ^3}{(TrQ^2)^{3/2}} \right\rangle, \tag{26}$$

where the average here is over different instantaneous measurements of Q during the simulation. This quantity is a measure of the degree of collinear spin-nematic order. It is zero for randomly oriented spins and increases as one approaches and enters the ordered phase, taking the value one in the well-ordered limit. It is thus a good quantity for doing a finite-size scaling analysis of the phase transition, as we show below. Note that the average value of the third power TrQ^3 of the order parameter does not vanish in this model. This reflects the fact that its Landau theory has a cubic term and thus the phase transition is expected to be of first order, just as in the case of the isotropic-to-nematic transition in 3D liquid crystals.

C. Phase diagram and the order of the transition

We first establish the existence of the ordered phase. We simulate the system with sizes $N_t = 8$, $N_x = 4,5,6,7$ for K_0

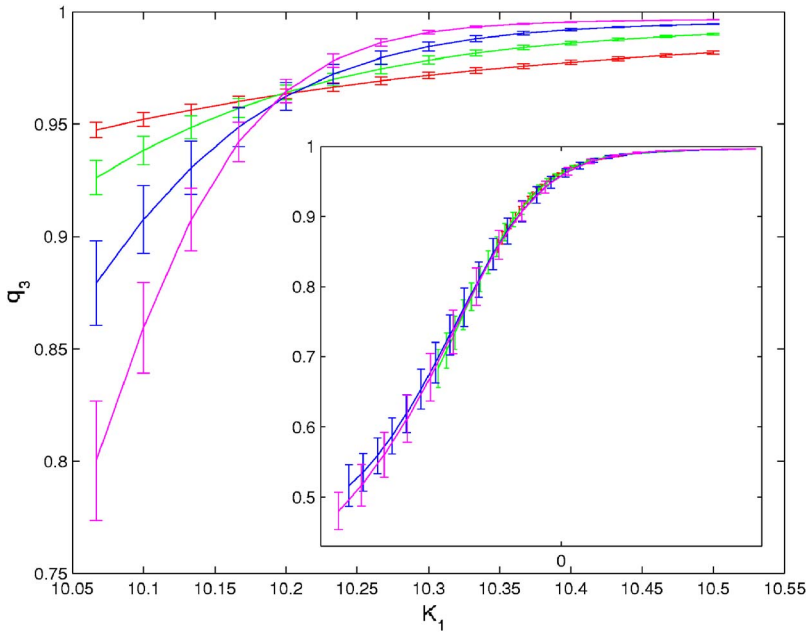

FIG. 6. (Color online) The values of q_3 for sizes $N_x=4,5,6,7$ (as N_x increases, the curves become steeper). The curves cross at one point, which is the estimated location of the phase transition. The inset shows q_3 plotted vs the scaling variable $(K_1-K_{1c})N_x^3$ appropriate for a first-order transition.

$=3$ and $K_1=10.1$ or $K_1=10.2$. In the process, for every configuration in the run, we save the "action" S_0 due to the couplings along the imaginary time direction and S_1 due to the space direction. This allows us to obtain estimates of q_3 for not only the values of the couplings simulated, but also for nearby values of the couplings by giving each spin configuration its Boltzmann weight $e^{K_0S_0+K_1S_1}$ in calculating the averages of q_3.

The results for q_3 for $K_0=3$ and a range of K_1 near the phase transition are shown in Fig. 6. A crossing of the curves for the different sizes is clearly seen at the estimated "critical" value of $K_{1c}\cong 10.20$.

Next we find how the order parameter scales with the size of the system. We rescale $(K_1-K_{1c})\rightarrow(K_1-K_{1c})N_x^{1/\nu}$ and tune ν to see when the curves of q_3 for different sizes align. We find that they align well for $\nu=1/3$, as shown in the inset to Fig. 6. Thus we can write $q_3=f[(K_1-K_{1c})N_x^d]$ where $d=3$ is the dimension of the system. This is the scaling expected for a first-order phase transition.

To give further evidence for the first-order phase transition, we calculate the furthest point correlation function defined as follows

$$\frac{3}{2}\langle(\vec{n}_{t,x,y,z}\cdot\vec{n}_{t+N_t/2,x+N_x/2,y+N_y/2,z+N_z/2})^2\rangle-\frac{1}{2} \qquad (27)$$

where the average is over all spins at one instant during the simulation. If the transition were first order, the finite size system at the transition point would jump back and forth between the ordered and disordered phase. Thus if we plot the histogram of these correlations we should see two peaks. These should get sharper as we increase the size of the system. The numerical results are shown in Fig. 7 where we indeed see two peaks, which are getting sharper with increasing size. These results, combined with our expectations from the Landau theory and the finite-size scaling of q_3 give strong evidence that the transition is first order. The place where we are showing this corresponds to a g near the maximum of T_c, but we expect this first-order character will also remain elsewhere on the phase boundary, including at the $T=0$ quantum phase transition at g_c.

Now that we have explored one point in the phase diagram, we would like to look at more of them and find the shape of the phase transition curve. In order to simplify the calculations we will look only for one size $N_x=5$, $N_t=8$ and say that the point is a point of phase transition if its q_3 value is the same as that at the crossing point in Fig. 6. Finding a point sufficiently close to the phase transition curve we reweight configurations as described above to find a point with this value of q_3. The results are shown in Fig. 8. The range that is readily accessible to our numerical simulations corre-

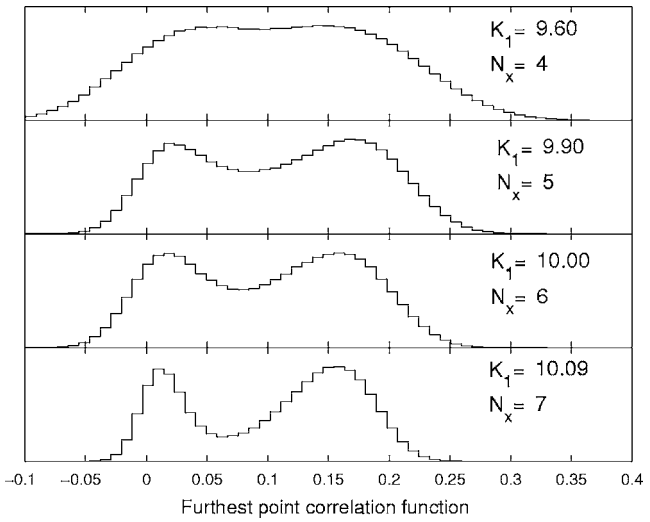

FIG. 7. Probability distributions of the furthest-point correlation function for $N_t=8$, $K_0=3$ at the values of K_1 where the two peak heights match. The peaks become sharper and the minimum in between deeper with increasing system size, as expected for a first-order transition.

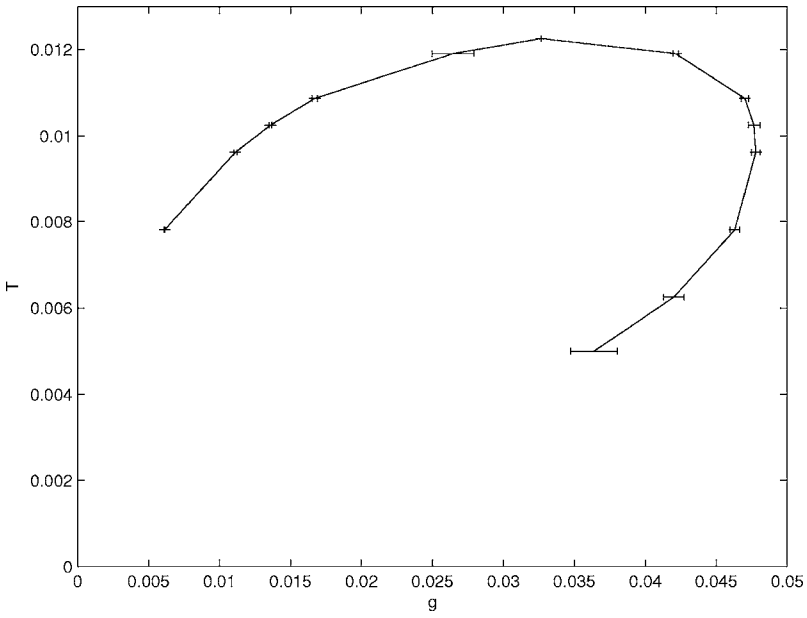

FIG. 8. The estimated phase transition curve for the $N_t=8$, $N_x=5$ system. The strong reentrance at low T on high g side of the phase diagram is likely an artifact of the very coarse imaginary time slicing that is done there with these parameters.

sponds to the higher temperature part of the phase boundary. We see that it has qualitatively the same shape as that of our single tetrahedron crossover diagram, and in particular it shows the reentrant behavior on varying g at a fixed T (in practice this is varying K_0 at a fixed K_1). The strong reentrance also seen at low T on the high g side of the phase diagram is likely an artifact of the very coarse imaginary time slicing that is done there with these parameters. We note that the transition temperature is very low, its maximum value is roughly $\sim 0.012J$ ($J=1$ in this paper); this low value is another manifestation of the strong frustration in this system.

V. LARGE n ANALYSIS

Our primary focus in this paper has been the physics of ordering via quantum fluctuations. As we have seen, this is a delicate effect which exists in a small corner of the (g,T) plane and one that goes away as $n\to\infty$.

This last observation suggests that in order to compute the properties of the system *away* from the region of ordering it is useful to resort to the large n approach. Indeed this observation has already been used in the classical limit, where ordering is absent for all $n\geqslant 3$, to obtain a very accurate theory of the spin correlations.[6,21] We will now extend this analysis to the quantum problem.

A brief recap of the analysis: We write the partition function as a path integral and impose the fixed length constraint by introducing a Lagrange multiplier field. The resulting action is quadratic in spins which can then be integrated out to obtain an effective action for the Lagrange multiplier field with an overall coefficient of order n which thus enables a saddle point treatment. The saddle point condition, which is all we need to solve to find the $n=\infty$ correlations, takes the form

$$\frac{1}{2N}\sum_{q,\sigma}\frac{\sqrt{g/2}}{\sqrt{\mu_q^\sigma+\lambda}}\coth\left(\frac{\sqrt{g/2}}{2T}\sqrt{\mu_q^\sigma+\lambda}\right)=1 \tag{28}$$

where λ is the uniform, saddle point value of the Lagrange multiplier field, σ runs over the four bands of the pyrochlore lattice and μ_q^σ are the eigenvalues of the adjacency (interaction) matrix for a lattice of N sites. As the lowest two bands are flat, with μ^σ independent of $\mathbf{q}$, this equation has a solution with $\lambda>0$ for any nonzero value of g and T. Hence the system is always disordered at $n=\infty$, consistent with our earlier considerations.

We will not write the resulting correlations of the spins explicitly. Instead it is instructive to write the correlations of the field that is obtained from them as follows. Let $\vec{n}$, defined at any site, be a vector pointing from one tetrahedron to the other (this can be chosen consistently as the tetrahedra surround sites of the bipartite diamond lattice). Then, for each component of the spin S, define the vector field $\vec{B}^a(x)=\vec{n}(x)S^a(x)$. The significance of this field lies in the fact that it has zero lattice, and thus coarse-grained, divergence in the classical ground state manifold. As discussed in Ref. 6 this field exhibits dipolar correlations in the $T\to 0$ limit in the classical problem. In our more general problem, at small g, T and q, we find that the retarded ground state correlations are

$$\langle B_i^a(q,\omega)B_j^b(-q,-\omega)\rangle_R = \delta^{ab}\left(\frac{\delta_{ij}q^2-q_iq_j}{q^2}\frac{g}{-\omega^2+\lambda' g}+\frac{q_iq_j}{q^2}\frac{g}{-\omega^2+g(\lambda'+q^2)}\right), \tag{29}$$

where we have ignored, for simplicity, numerical factors that appear in front of g and λ' $(=\lambda-1)$. From the saddle point condition for $T\ll g\ll 1$, $\lambda'\sim g$ and for $g\ll T\ll 1$, $\lambda'\sim T$. The crossover occurs at $T\sim g$. We expect that this formula describes the correlations away from very small g and T in the disordered phase rather well. We should emphasize that this covers the bulk of the strongly correlated or cooperative paramagnetic regime, $T,g\ll J=1$, where the correlations between the rotors are significant although the system is still disordered.

These forms reduce at equal times and $g=0$ to the dipolar forms derived in Ref. 6 At zero T and nonzero g we see that the correlations decay exponentially in space with a correla-

tions length of order $g^{-1/2}$ and exponentially in time with a gap of order g. Observe that the $n=\infty$ problem does not contain any trace of the nematic ordering that exists at finite n. Individual terms in the $1/n$ expansion for the correlation function can be seen to be well behaved[22] and so while they can be used to obtain a more accurate treatment of the cooperative paramagnetic regime, it will take an analysis of the series to reproduce the instability that we have obtained earlier. This is a challenge for future work.

VI. CONCLUSIONS

We have fully explored the local ordering of a single tetrahedral unit of four neighboring rotors. They order collinearly, with two rotors pointing along one direction and the other two in the opposite direction. Thus an *axis* of ordering is chosen, and since in the full pyrochlore lattice this tetrahedron shares one rotor with each of its neighbor tetrahedra, this axis of ordering is uniform throughout the lattice in the ordered phase, which thus has spin-nematic, or collinear order. We have demonstrated this spin-nematic ordering within a quantum Monte Carlo simulation. There might also be long-range order in which rotors point in which direction along this axis, and/or in which pairs of rotors are parallel or antiparallel. We have not yet been able to determine whether our ordered phase has any of these latter types of sublattice order in addition to its collinear order. We find that the collinear order shows up quite robustly in our quantum Monte Carlo simulations, while any other long-range correlations that might be present appear to be much weaker and difficult to detect, if they are indeed there.

We note that the considerations outlined here apply straightforwardly to the two-dimensional checkerboard lattice which is the planar analog of the pyrochlore lattice. By contrast an analysis of the rotor models on the kagome lattice will require a fresh analysis.

ACKNOWLEDGMENTS

We thank Roderich Moessner for valuable discussions and the NSF for support through MRSEC Grant No. DMR-0213706.

[1] R. Moessner, Can. J. Phys. **79**, 1283 (2001).
[2] A. P. Ramirez, Annu. Rev. Mater. Sci. **24**, 453 (1994).
[3] See, e.g., the references mentioned at http://www.pha.jhu.edu/~olegt/pyrochlore.html for representative examples.
[4] R. Moessner and J. T. Chalker, Phys. Rev. Lett. **80**, 2929 (1998); R. Moessner and J. T. Chalker, Phys. Rev. B **58**, 12049 (1998).
[5] The pattern of the spin ordering is not known.
[6] S. V. Isakov, K. Gregor, R. Moessner, and S. L. Sondhi, Phys. Rev. Lett. **93**, 167204 (2004); C. L. Henley, Phys. Rev. B **71**, 014424 (2005).
[7] C. L. Henley, Phys. Rev. Lett. **96**, 047201 (2006); U. Hizi and C. L. Henley, Phys. Rev. B **73**, 054403 (2006).
[8] A. B. Harris, J. Berlinsky, and C. Bruder, J. Appl. Phys. **69**, 5200 (1991).
[9] H. Tsunetsugu, J. Phys. Soc. Jpn. **70**, 640 (2001).
[10] H. Tsunetsugu, Phys. Rev. B **65**, 024415 (2001).
[11] A. Koga and N. Kawakami, Phys. Rev. B **63**, 144432 (2001).
[12] B. Canals and C. Lacroix, Phys. Rev. Lett. **80**, 2933 (1998).
[13] E. Berg, E. Altman, and A. Auerbach, Phys. Rev. Lett. **90**, 147204 (2003).
[14] Y. Yamashita, K. Ueda, and M. Sigrist, J. Phys.: Condens. Matter **13**, L961 (2001).
[15] O. Tchernyshyov, R. Moessner, and S. L. Sondhi, Europhys. Lett. **73**, 278 (2006).
[16] R. Moessner, S. L. Sondhi, and M. O. Goerbig, Phys. Rev. B **73**, 094430 (2006).
[17] See, for example, S. Sachdev, *Quantum Phase Transitions* (Cambridge University Press, Cambridge, 1999); also, J. Ye, S. Sachdev, and N. Read, Phys. Rev. Lett. **70**, 4011 (1993); N. Read, S. Sachdev, and J. Ye, Phys. Rev. B **52**, 384 (1995) in the context of spin glasses.
[18] R. Moessner, S. L. Sondhi, and P. Chandra, Phys. Rev. Lett. **84**, 4457 (2000); R. Moessner and S. L. Sondhi, Phys. Rev. B **63**, 224401 (2001).
[19] The robust existence of the quantum paramagnetic phase makes rotors quite different from spins where large quantum fluctuations do not select a unique state. One can, however, consider modified rotor models where monopoles placed at the centers of rotors modify their low energy spectra. Such a rotor model is, for example, the lattice representation of the $O(3)$ nonlinear sigma model with a topological term in $d=1+1$ [R. Shankar and N. Read, Nucl. Phys. B **336**, 457 (1990)].
[20] The probability distribution becomes more and more concentrated on collinear configurations as $T\rightarrow 0$. Of course there is no spontaneous symmetry breaking in this finite system.
[21] B. Canals and D. A. Garanin, Can. J. Phys. **79**, 1323 (2001).
[22] K. Gregor, D. A. Huse, and S. L. Sondhi (unpublished).